Estimation of Location and Coordinated Tuning of PSS based on Mean-Variance Mapping Optimization

J. L. Rueda, *Member, IEEE*, J. C. Cepeda, *Graduate Student Member, IEEE*, and I. Erlich, *Senior Member, IEEE*

***Abstract*--Proper location and adjustment of power system stabilizers (PSSs) is of great concern to achieve effective enhancement of overall power system damping performance. Thus, the problem of optimal location and coordinated tuning of PSSs (OLCTP) requires the fulfillment of several specifications to ensure system operation with adequate security margins for different operating conditions. This paper presents a comprehensive approach to tackle the OLCTP based on a combination of probabilistic eigenanalysis (PE) and the mean-variance mapping optimization (MVMO). PE is employed to assess the probabilistic attributes of the system eigenstructure associated to the statistics of nodal injections. Next, a combined technique of principal component analysis and fuzzy c-means clustering is applied to select a reduced subset of relevant scenarios to be considered in the formulation of the OLCTP. The number of PSSs, as well as the set of parameters that ensure robustness for operating condition change, are determined through MVMO. Numerical results demonstrate the effectiveness of the proposed approach. In addition, an adaptive controller coordination scheme, which can be used online, is suggested.**

***Index Terms*--Small-signal stability, power system stabilizer, probabilistic eigenanalysis, heuristic optimization.**

I. Introduction

With the changing ways that power systems are being operated in the power industry deregulated environment, poorly damped low-frequency electromechanical oscillations may restrict the maximum power transfer limits, which also entails adverse implications for system security and economics [1]. From power system operation perspective, much work has been directed towards the development of methods for improving system small-signal stability performance through operational strategies such as generation rescheduling methods [2] and coordination of transmission path transfers [3]. Other innovative methods suggest optimal power flow computation including small-signal stability constraints [4] and computational intelligence based optimal adjustment of power flow and bus voltage features [5].

Also, considerable effort has gone into the research area of supplementary damping controllers. The power system stabilizer (PSS) has been proposed as supplementary excitation controller to damp out troublesome oscillations, thereby enhancing the overall system stability while extending the transfer capability limits. Hence, PSSs have proved to be a simple, effective, and economic control option and therefore extensively used by utilities [6].

Mathematically, the unified solution to the PSS location and robust tuning problems can be quite complex in multi-machine power systems with changing operating conditions. On one side, the PSS location problem has been a subject of intensive research over the last two decades. Many approaches and indexes based on participation factors, residues, damping torque, sensitivity coefficients and singular value decomposition have been reported for identifying suitable PSS locations [7], [8]. Relationships between some of these approaches have been discussed in [9] and a comparative study is presented in [10]. Notwithstanding, they are based on a deterministic framework. Several studies extent the conventional sensitivity coefficient analysis to the probabilistic context in order to determine probabilistic sensitivity indexes for selecting PSS locations [11]. However, these studies are based on analytical probabilistic approaches which may provide misleading estimates of eigenvalue statistics due to extensive underlying assumptions. This disadvantage becomes more evident when considering large-size power systems with a high number of uncertain input variables [12].

Likewise, there is a myriad of methods that have been devised for PSS tuning. The first methods were based on the synthetic single machine - infinite bus bar scheme [13]. However, due to the inherent limitations of this type of approach, the resultant PSSs were not always effective in multimachine systems with widely varying operating conditions. Therefore, some proposals for multimachine models based on fuzzy-logic systems [14], artificial neural networks [15], H∞ robust control [16], and meta-heuristics [17], to name a few, have been reported, aiming to robust PSS designs. Recent efforts have also been made to attempt a unified solution for both problems of optimal PSSs' location and parameter definition [18]-[20]. In this connection, this

This work was supported by the German Academic Exchange Service, the University Duisburg-Essen and the Universidad Nacional de San Juan.

J. L. Rueda and I. Erlich are with the Department of Electrical Power Systems, University Duisburg-Essen, Duisburg, 47057, Germany (e-mail: jose.rueda@uni-duisburg-essen.de, istvan.erlich@uni-due.de).

J. C. Cepeda is with Instituto de Energía Eléctrica, Universidad Nacional de San Juan, San Juan, 5400, Argentina (e-mail: jcepeda@iee.unsj.edu.ar).

978-1-4673-2729-9/12/$31.00 ©2012 IEEE

paper proposes a comprehensive approach to tackle the problem of simultaneous determination of optimal locations and coordinated tuning of PSSs (OLCTP). Firstly, probabilistic eigenanalysis (PE) is employed to assess the probabilistic attributes of the system eigenstructure associated to the statistics of nodal injections. Next, a combined technique of principal component analysis (PCA) and fuzzy c-means clustering (FCM) is applied to select a reduced subset of relevant scenarios to be considered in the formulation of the OLCTP, which is solved by mean-variance mapping optimization (MVMO). The results obtained using the IEEE New England test system highlight the viewpoint and effectiveness of the proposed approach. Since MVMO falls into the category of the so-called population-based stochastic optimization techniques, its performance is compared with that of a standard particle swarm optimization (PSO). Furthermore, an intelligent scheme for adaptive controller coordination is outlined.

The remaining part of the paper is organized into the following sections: Section II gives an overview of the proposed approach, discussing the main issues associated with PE and MVMO. In Section III, a test case is developed and evaluated. Finally, conclusions and outlook for future work are drawn in Section IV.

II. Proposed Approach

The framework of the proposed approach is sketched schematically in Fig. 1. It starts with the definition of the models required for power system steady-state and dynamic analysis (i.e. actual system model), the probabilistic models (i.e. probabilistic distribution functions -PDFs) of input system variables and the requirements imposed on the system by the small-signal stability constraint in order to guarantee secure operation. Next, PE is performed to assess the probabilistic properties of the system eigenstructure (i.e. eigenvalues, eigenvectors and participation factors) with respect to changing operating conditions (e.g. random variation of nodal injections). In the subsequent stage, a combined technique of PCA and FCM is employed to exploit the insights gained from PE in order to select a subset of relevant scenarios which are accounted in the formulation of the OLCTP. Finally, optimal PSSs' location and parameters are determined through MVMO.

A. Probabilistic eigenanalysis

The flowchart of the PE method is illustrated in Fig. 2 [21]. It resembles a Monte Carlo (MC) type repetitive simulation, which requires previous definition of the probabilistic models of system input variables (i.e. probability distribution functions - PDFs). The MC-based PE procedure starts with a sampling strategy to draw random samples of input variables in consistency with their PDFs. Next, based on a settled utility's operating policy to balance power (e.g. least-cost or merit-order economic dispatch), a set of generation variables corresponding to each set of sampled nodal demands is obtained (i.e. all components of the nodal injection vector are obtained). Each trial nodal injection vector defines an operating state that is determined by power flow calculation.

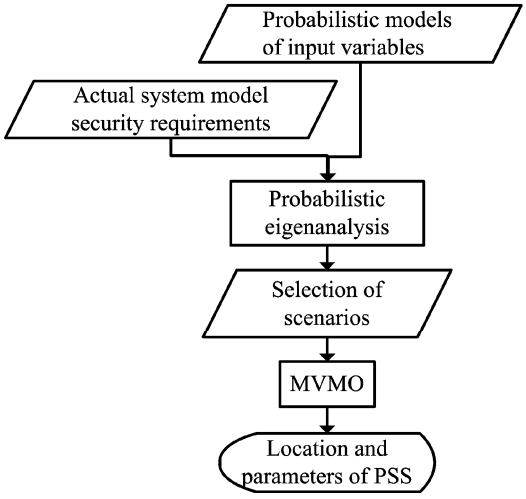

Fig. 1. Framework of the proposed approach

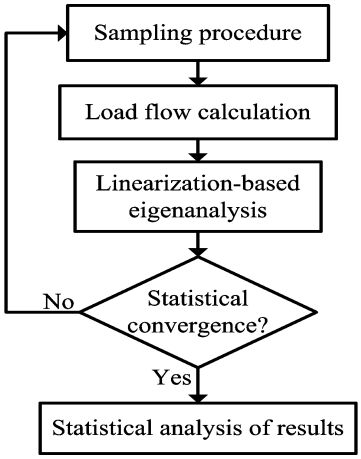

Fig. 2. Monte Carlo-based probabilistic eigenanalysis

Viable operating states (which fulfil steady-state voltage limits, thermal overloading of transmission elements, and maintain the generation units operating within their limits) as well as operating states characterized by overloading of transmission network elements and low voltage profiles are then selected. Next, for each selected operating state, the system small-signal stability is evaluated via linearization-based eigenanalysis [22]. Here, critical oscillatory modes (OMs), their associated frequency, damping ratio ζ, right and left eigenvectors as well as participation factors are calculated. An eigenvalue tracking procedure based on modal parameters is also applied at this stage to ensure proper storage of modal analysis information and to ensure proper statistical evaluation of computed critical mode parameters. Besides, sequential estimation of statistical relative error is applied in order to ensure a high degree of confidence of the eigenvalue statistics. Thereafter, based on the resultant statistics, the mean, variance, skewness and kurtosis parameters as well as histograms and boxplots can be used to describe the variability of the system eigenstructure. Besides, the

probabilistic indexes R_{Inst} and DE_{PSS} are calculated to assess the instability risk due to negatively damped or lowly damped OMs and to provide suggestive PSS location. Based on a defined ζ threshold (e.g. $\zeta_{th} > 5\%$), the R_{Inst} index is calculated accounting the cumulative PDF associated to each critical mode ζ as follows

$$R_{\text{Inst}} = \begin{cases} \text{OM}_{\zeta\text{-Neg}} = \text{P}(\zeta_i < 0) \\ \text{OM}_{\zeta\text{-Poor}} = \text{P}(0 \le \zeta_i < 5\%) \\ \text{OM}_{\zeta\text{-Damp}} = \text{P}(\zeta_i \ge 5\%) \end{cases} \text{i} = 1, \cdots, \text{M}_\text{C} \quad (1)$$

where $OM_{ζ\text{-Neg}}$ indicates the probability of instability due to negatively damped OM, $OM_{ζ\text{-Poor}}$ indicates the probability associated to poorly damped OM, and $OM_{ζ\text{-Damp}}$ indicates the probability associated to well damped OM. M_C is the number of critical modes, and P(.) denotes cumulative probability.

Considering different critical modes separately, and through the analysis of the histograms of the participation factors, the DE_{PSS} index is computed for each mode according to:

$$\text{DE}_{\text{PSSi}} = \max_{\text{k}=1\cdots\text{N}_\text{G}} \left\{ \text{E}\left| pf_{\Delta\omega} \right|_\text{k} \right\} \quad (2)$$

where the suffix i denotes the i-th mode, N_G is the number of generators, $E|pf_{Δω}|$ is the mean of the participation factor (*pf*) associated with the generator speed deviation states (Δω).

B. Selection of scenarios

The several random scenarios defined by MC cannot be jointly used in the formulation of the OLCTP due to the huge complexity of the optimization process, which, indeed, would entail a tremendous computational burden. Hence, a reduced number of scenarios must be chosen. These scenarios have to effectively represent all the possible operating states embraced by the probabilistic simulation. Thus, a combined technique of PCA and FCM is applied to properly select the reduced subset of relevant scenarios to be considered in the formulation of the OLCTP, which constitute the input of the MVMO algorithm.

The *n* operating scenarios generated by MC simulation (i.e. observations) are represented by multivariate vectors of *p* features, which include active and reactive power nodal injections, as well as the frequency and damping of the poorly damped OMs. The feature vector set constitutes a ($n \times p$) multivariate data matrix (*X*).

Performing multivariate analysis to the data matrix allows technically determining clusters of possible operating states, whose centroid features can be considered as representative of all possible scenarios. Firstly, univariate normalization is carried out to the data matrix for avoiding the influence of different measurement units of original variables. This normalization converts the original variables in other new ones with zero mean and unit variance.

Then, PCA is applied to the normalized data matrix in order to reduce the dimensionality of the data, maintaining as much as possible of the variation presented in them. This is achieved by transforming the data to a new set of variables, the principal components (PCs), which are uncorrelated and ordered so that the first few components keep most of the variation present in the original variables [23]. The sum of the PC eigenvalues ($λ_i$) is equivalent to the total variance of the data matrix, and each PC eigenvalue offers a measure of the corresponding explained variability (EV_i). So, the number of the chosen PCs depends on the desired explained variability, which is specified as more than 90% in this paper (3).

$$\text{EV}_\text{i} = \frac{\lambda_\text{i}}{\sum_{i=1}^{p} \lambda_\text{i}} \times 100 \quad (3)$$

Next, FCM is applied to the first PC scores in order to determine the clusters of the operating states. Finally, the feature vectors that have the minimum Euclidean distance to the cluster centroids are chosen as the representative scenarios.

C. Optimal location and coordinated tuning of PSSs

A PSS is generally viewed as an additional block of a generator excitation control. The block diagram of a typical PSS is shown in Fig. 3. Typically, the PSS uses a stabilizing feedback signal such as, for instance, generator shaft speed ($ω_{shaft}$), to modulate the reference of the automatic voltage regulator [22]. The PSS input signal is first passed through a high-pass filter (commonly termed washout filter) which prevents input's steady state changes from modifying the field voltage. The phase compensation blocks provide the appropriate phase-lead characteristic to compensate for the phase lag between the exciter input and the generator electrical torque. The stabilizer gain block determines the amount of damping introduced by the PSS [6].

From the washout function perspective, the value of the associated time constant T_W is not critical, since it should be considered small enough such that stabilizing signals at the frequencies of interest will be relatively unaffected. Thus, T_W is considered known beforehand (e.g. T_W = 10s) [22], [24]. Therefore, a reasonable overall damping performance during the system upsets (i.e. maximising the damping ratios while avoiding destabilizing interactions between PSSs) is related to the appropriate determination of the number, location and remaining parameters of the PSSs (i.e. gain K_{PSS} and time constants T_1 to T_4).

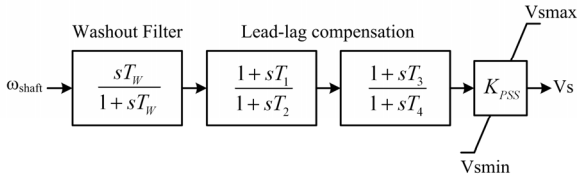

Fig. 3. Typical PSS structure

C.1. OLCTP problem statement

To tackle the aggregate problem of deciding on the location and tuning of the PSSs while minimizing the number of controllers and achieving a satisfactory overall system damping performance for all OMs and for all the relevant scenarios determined in the previous stage, an optimization

problem can be defined as follows [25]:

$$\min \mathrm{OF}(\mathbf{x}) = \sum_{k=1}^{nc}\sum_{i=1}^{nm}\sum_{j=1}^{ng}\left(1\text{-}p_{ij}\right)\mathrm{K}_{PSSj} \tag{4}$$

subject to

$$\mathbf{x}_{j-\min} \le \mathbf{x}_j \le \mathbf{x}_{j-\max} \tag{5}$$

$$\zeta_i \ge \zeta_{th} \tag{6}$$

$$\left|\Delta f_i\right| \le \Delta f_{th} \tag{7}$$

where $\mathbf{x}$ is the solution to the problem, that is, the set of control variables (gain K_{PSS}, and time constants T_1 to T_4) to be determined for each PSS to be installed. K_{PSSj} is the PSS gain of the j-th generator, p_{ij} is the normalized speed participation factor of the j-th generator in the i-th OM, nc is the number of selected scenarios, nm is the number of OMs, and ng is the number of generators.

The objective function, as defined in (4), constitutes a weighted sum of the PSSs' gains. The weighting coefficients are defined in terms of normalized participation factors of generator speed deviation states (p_{ij}), which can be seen as the mode sensitivity to the installation of an ideal PSS using speed input [25]. Thus, for instance, if only the j-th generator has influence on the i-th mode, then $p_{ij} = 1$, which implies a null weighting coefficient and also means that the PSS gain of that generator can take any value between its limits. By contrast, if $p_{ij} = 0$ or $p_{ij} = -1$, it is because the j-th generator has no influence or has dampening effect over the i-th mode, which entails a non-zero weighting coefficient, meaning that the PSS gain of that generator will be minimized. Note that those where the gain of the PSS has a non-zero values are the ones to be selected for PSS location.

The constraint (5) imposes minimum and maximum limits to the gains and the time constants in the lead-lag blocks of the PSSs, whereas, according to constraint (6), the damping ratio of the OMs is to be set above the minimum acceptable threshold (e.g. $\zeta_{th} > 5\%$), which ensures that these modes have sufficient damping and considerable stability margin. According to constraint (7), frequency excursions of the OMs should be limited within a narrow range in order to ensure that the system transient stability margins will not be adversely affected [6].

The determination of the solution to this optimization problem is handled, in this paper, through MVMO, which was originally proposed in [26] and shares certain similarities to other heuristic approaches, but possesses a special mapping function. In power system optimization, MVMO has been successfully applied to solve the optimal reactive power dispatch problem [27]. In [28], numerical comparisons between MVMO and some basic and enhanced evolutionary algorithms show that MVMO exhibits a better performance, especially in terms of convergence speed.

C.2. Mean-variance mapping optimization

The MVMO operates on a single solution rather than a set of solutions like in many evolutionary algorithms. The internal searching space of all variables in MVMO is restricted in [0,1]. Hence, the real min/max boundaries of variables have to be normalized to 0 and 1. During the iteration it is not possible that any component of the solution vector will violate the corresponding boundaries. To achieve this goal, a special mapping function is developed. The inputs of this function are mean and variance of the best solutions that MVMO has discovered so far. The elegant property of MVMO is the ability to search around the local best-so-far solution with a small chance of being trapped into one of the local optimums. This feature is contributed to the strategy for handling the zero-variance [26]. The procedure of MVMO for solving the OLCTP problem with D variables is summarized in Fig. 4.

Step 1:	Read power system data and set MVMO parameters.
Step 2:	**Initialization:** Initialize an initial vector $\mathbf{x}$ in [0,1] based on the uniform random distribution.
Step 3:	**Fitness evaluation:** De-normalize $\mathbf{x}$, run the power flow and evaluate the fitness function.
Step 4:	**Termination:** Check the termination criteria. If yes, terminate MVMO. Else, **continue** to step 5.
Step 5:	**Solution archive:** Store $\mathbf{x}$, fitness value, objective value and feasibility to the archive if $\mathbf{x}$ is better than any of existing solutions.
Step 6:	Based on the archived solutions, compute mean $\overline{x}_i$ and variance v_i for each dimension *i*.
Step 7:	**Parent assignment:** Assign the best archived solution $\mathbf{x}_{best}$ as the parent.
Step 8:	Variable selection: Select $m < D$ dimensions of $\mathbf{x}$.
Step 9:	**Mutation:** Apply the mapping function to the selected *m* dimensions.
Step 10:	**Crossover:** Set the remaining *D-m* dimensions of $\mathbf{x}$ to the values of $\mathbf{x}_{best}$
Step 11:	Go to step 3.

Fig. 4. MVMO implementation procedure for OLCTP

III. Test Results

Numerical experiments were performed on a Hewlett Packard Pavilion dv3 personal computer with an Intel® Core™ 2 central processing unit (CPU), 2.2 GHz processing speed, and 4GB RAM. The simulation environments MATLAB®, MATPOWER© [29], and DigSILENT Power Factory© were used to accomplish the implementation aspects and to test the proposed approach. The implicit restarted Arnoldi method is used for fast eigenvalue computation. The approach is tested using the IEEE New England 39 bus test system [30], whose single line diagram is depicted in Fig. 5. All generators are represented by sub-transient model and equipped with excitation systems as well as thermal turbine governor systems. Changes have been made in the system to account for different operating conditions characterized by considering multivariate normal PDF representing nodal demand uncertainties around highly loaded conditions. Besides, mean values of the coefficients defining piecewise quadratic cost functions of generating units were considered.

A. Probabilistic study and selection of scenarios

Initially, no PSSs were considered in order to study the system damping performance without the addition of supplementary damping controllers. Overall CPU time for PE with 11,734 trials is 3.78 h. A set of nine critical modes was registered in all analyzed operating states and the statistics of their frequencies and damping ratios are summarized in Table I. The lowest frequency mode 1 is an inter-area mode in which generator 1 (which is modeled as a single large generator representing an aggregated equivalent of the New York system) oscillates against the rest of the system generators. The higher frequency OMs are intra-area and local modes.

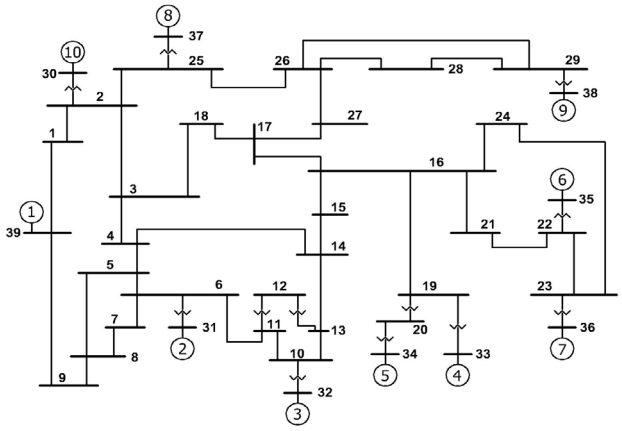

Fig. 5. IEEE New England 39 Bus test system

TABLE I
STATISTICS OF CRITICAL OMS

		Freq. (Hz)		Damping (%)	
Mode	**Generator**	**Mean**	**Std**	**Mean**	**Std**
1	All	0.6165	0.0056	6.3350	0.2163
2	G2	0.9080	0.0133	3.5522	0.1339
3	G3	1.0578	0.0199	4.8024	0.1996
4	G4 to G8	1.3776	0.0137	4.0521	0.1503
5	G5,G6	1.1688	0.0039	3.8369	0.0223
6	G4 to G7	1.4061	0.0065	3.7717	0.0546
7	G8	1.2719	0.0076	5.7319	0.4801
8	G9	0.9842	0.0130	4.3695	0.1554
9	G10	1.7986	0.0075	6.7686	0.1379

It is considered that the system has sufficient damping when the critical modes have $\zeta \geq 5\%$ for all operating conditions. Hence, according to the values for the three possibilities of R_{Inst} index summarized in Table II, there is a high small-signal instability risk associated with the occurrence of poorly damped oscillations. This is reasonable since the different rates of random increase in demand generated from the PDF around highly loaded conditions result in higher power flows over most of the long lines in the system, which would indeed deteriorate the system damping performance.

Based on PE results, relevant scenarios are established. Fig. 6 shows the spatial distribution of the three main PC scores and the clustering formation. In the figure, the three-dimensional PC scores are grouped into three different clusters using FCM algorithm. The red circles highlight the centroid locations, which can be considered as the three most representative scenarios among the whole number that was analyzed across MC-based PE by similarity judgment according to the statistical properties of their attributive features (i.e. system loading conditions and modal properties).

TABLE II
R_{INST} INDEX

Mode	**$OM_{\zeta\text{-Neg}}$**	**$OM_{\zeta\text{-Poor}}$**	**$OM_{\zeta\text{-Damp}}$**
1	0.00	0.01	0.99
2	0.00	1.00	0.00
3	0.00	0.77	0.23
4	0.00	1.00	0.00
5	0.00	1.00	0.00
6	0.00	1.00	0.00
7	0.00	0.02	0.98
8	0.00	1.00	0.00
9	0.00	0.00	1.00

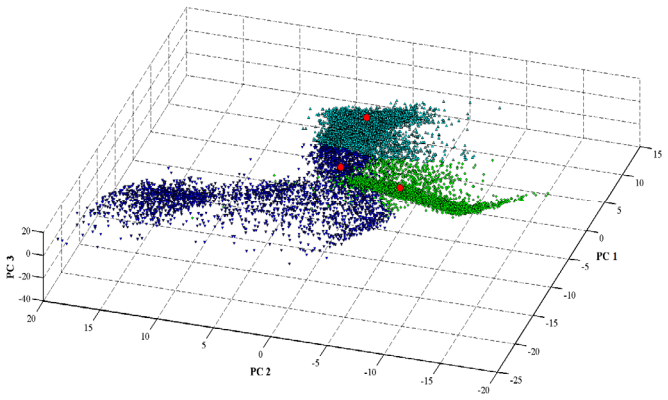

Fig. 6. Main PC scores and clustering formation

The DE_{PSS} index is computed for all critical modes according to equation (2) and the most suitable suggested PSS locations are summarized in Table III. From this perspective, most generators should be required to add a PSS, which could be not effective for operating condition change, as evidenced, for instance, in the boxplot of the speed deviation participation factor of mode 4 shown in Fig. 7. In the figure, the central mark of each box denotes the median, the edges of the box represent the 25% and 75% of the total data, the whiskers extend to the most extreme data points not considered as outliers (i.e. data with large deviation ranges from the mean value), and the blue triangles show the outliers plotted individually. Note that, from a purely maximum mean speed participation factor viewpoint, using the participation factor as an indicator for PSS location, G4 would be the most suitable option for increasing the damping of mode 4. Nevertheless, the statistical analysis demonstrates that G4 participation factor has the highest variability, showing greatest amount of outliers. Thus, the decision of PSS location using only the mean speed participation factor could not always provide an effective contribution to overall system damping performance. Therefore, in order to obtain a more confident decision, it is necessary to perform a coordinated optimization considering both the most relevant scenarios that properly represent probable operating conditions as well as the variability of the participation factors. Such an optimization problem was formulated in equations (4) to (7). The optimization results are

presented in the following subsection.

B. Optimization results

In addition to the scenarios selected in the previous subsection, the PSS parameters were adjusted considering typical limits, that is K_{PSS} = [0, 50], $T_1 = T_3$= [0.2 2], $T_1/T_2 = T_3/T_4$ = [1 30]. Therefore, the OLCTP search space has 45 dimensions. The population size of the PSO is set to 15. The convergence of the OF averaged from 10 independent trials of both MVMO and standard PSO [31] is shown in Fig 8. Note that, MVMO outperforms outstandingly the standard PSO in terms of both convergence speed and the minimum reached. This observation matches with one of the conclusions established in [28], since after the first 3,000 function evaluations, the MVMO is able to locate the optimal area in the search space. Moreover, it can continue exploring that area for any better solution without being trapped in one of local optimums.

TABLE III
DE_{PSS} INDEX

Mode	Generator	Mean speed PF
1	G6	0.48
2	G2	1.00
3	G3	1.00
4	G4	0.90
5	G5	1.00
6	G7	0.90
7	G8	1.00
8	G9	1.00
9	G10	1.00

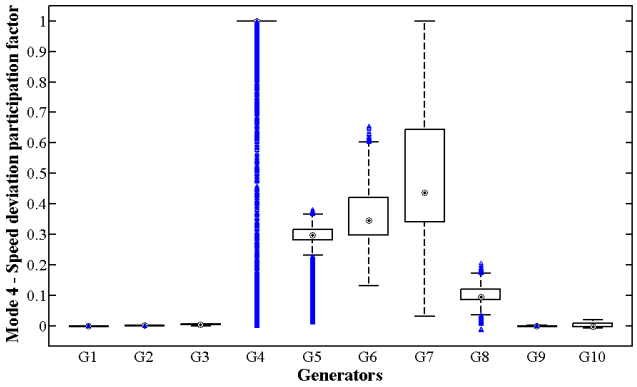

Fig. 7. Mode 4 – Speed deviation participation factor boxplot

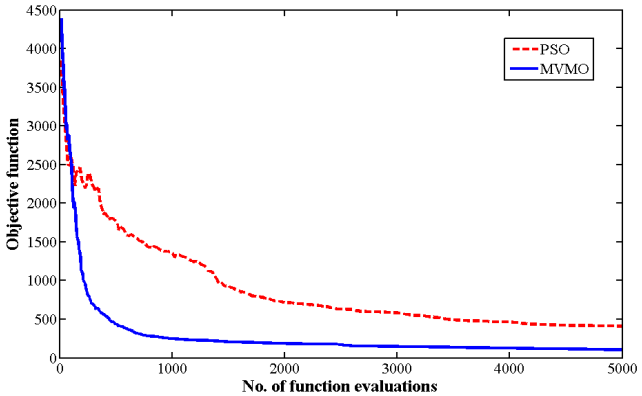

Fig. 8. PSO and MVMO average convergence characteristics

Besides, to fairly compare the quality of the final results obtained with both optimization techniques, the PSO was run for 16,500 function evaluations performed in 13.23 h whereas MVMO was run 5000 function evaluations that required 5.48 h. The OLCTP results, in terms of PSS location and gains, given by each method, are summarized in Table IV. Both techniques yield comparable gains but there are some differences in terms of PSS locations related to generators 4 and 8, which may be due to the variability of their speed participation factors which could be assimilated differently in the reproduction process (i.e. creation of new offspring) of both algorithms.

Based on one of the worst case among the representative scenarios, linearization-based eigenanalysis was performed to illustrate the small-signal performance of the system after adding PSSs according to both optimization results. Fig. 9 shows the frequency and damping ratio of each critical mode. It can be seen that satisfactory damping ratios can be achieved with both OLCTP results, but, by contrast, the mode frequency deviations are smaller for the MVMO case. Note also that the least-damped mode is obtained when the PSO results are used whereas most modes exhibit comparable damping ratios when using the MVMO. Time domain simulation was also performed here to further assess the quality of the obtained results. For this purpose, a three-phase fault was applied in bus 16 at 1.1 s with a duration of 50 ms. Fig. 10 presents the oscillograms corresponding to the active power flow of transmission line 9 – 39, showing comparable oscillatory shapes for both PSO and MVMO algorithms.

TABLE IV
PSS LOCATION AND GAINS

	PSO	MVMO
Generator	Mean	Mean
G2	0.948	3.131
G3	4.864	0.415
G4	Not used	0.214
G5	0.494	0.520
G6	0.311	0.449
G7	0.964	0.349
G8	1.627	Not used
G9	0.311	0.511
G10	Not used	Not used

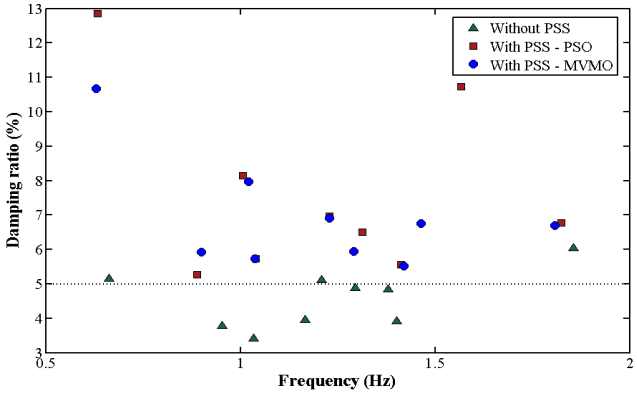

Fig. 9. Time domain simulation

C. Adaptive intelligent damping control

PE of the system was further performed in order to ascertain whether the system is small-signal secure throughout wide-ranging operating conditions. The values for the R_{Inst} index are presented in Table V, comparing the instability risk that arises when considering OLCTP results obtained with both MVMO and PSO. It can be seen that, although installing PSS according to MVMO perspective reduces considerably the instability risk, some operating states may still exhibit poorly OMs. On the other hand, the instability risk would be considerably higher for the PSO case. These results may be related to the PSSs' gains obtained either through MVMO or PSO, since the objective function pursues the smallest weighted sum of the PSSs' gains. Thus, future research work is being directed towards redefinition of the objective function as well as consideration of additional remote input signals. The results may also be attributed to the fact that, the solutions obtained with a reduced subset of relevant scenarios tend to be conservative due to the assumption that the solutions obtained for particular operating states can be satisfactory when the analysis extends to many different operating states. This aspect could be overcome by individually solving the OLCTP for several sets of representative scenarios in order to structure table based controller coordination.

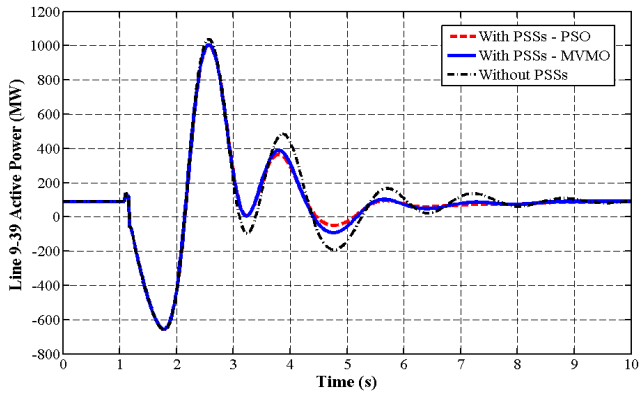

Fig. 10. Time domain simulation

TABLE V
COMPARISON OF R_{INST} INDEX AFTER PSS COORDINATED TUNING

OLCTP	R_{Inst}/Mode	1	2	3	4	5	6	7	8	9
MVMO	$OM_{\zeta\text{-Neg}}$	0.00	0.00	0.00	0.00	0.00	0.00	0.00	0.00	0.00
	$OM_{\zeta\text{-Poor}}$	0.00	0.26	0.05	0.41	0.38	0.17	0.00	0.09	0.00
	$OM_{\zeta\text{-Damp}}$	1.00	0.74	0.95	0.59	0.62	0.83	1.00	0.91	1.00
PSO	$OM_{\zeta\text{-Neg}}$	0.00	0.00	0.00	0.00	0.00	0.00	0.00	0.00	0.00
	$OM_{\zeta\text{-Poor}}$	0.00	0.49	0.08	0.58	0.45	0.33	0.00	0.22	0.00
	$OM_{\zeta\text{-Damp}}$	1.00	0.51	0.92	0.42	0.55	0.67	1.00	0.78	1.00

For on-line applications, the proposed approach could be combined with knowledge-based pattern recognition techniques to structure the function of an adaptive intelligent damping control coordinator, whose implementation procedure can be summarized as shown in Fig. 11. The input features are a set of real-time monitored system signals describing the actual operating state. PCA is then applied for input dimensionality reduction. The information obtained off-line from PE and OLCTP serves as a system knowledge base which can be used for two key purposes, namely: i) to train an intelligent classifier (e.g. Support Vector Machine Classifier) that enables determining the security status of the actual operating state, and ii) to synthesize the relationships between varying sets of representative system states and optimal parameters (i.e. non-linear mapping from the space of actual system state to the space of coordinated control parameters).

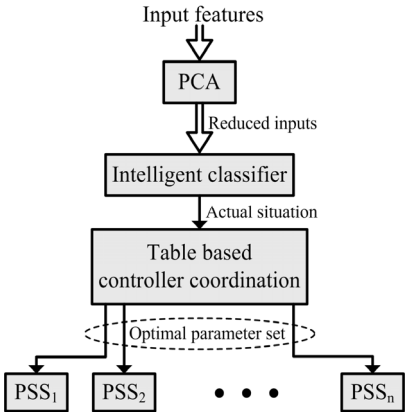

Fig. 11. Adaptive controller coordination scheme

IV. CONCLUSIONS

In this paper, a comprehensive approach for solving the OLCTP using a combination of PE, PCA, FCM and the MVMO is presented. The main premise was to ensure an effective improvement of the overall system dynamic performance by determining the location and tuning of the PSSs while minimizing the number of controllers. Numerical results highlight the importance of solving the OLCTP considering both the most relevant scenarios that properly represent probable operating conditions as well as the variability of the system eigenstructure. The adoption of the MVMO to deal with the optimization task has further confirmed its outstanding performance both in terms of convergence and the minimum reached. This property is of great value, since the OLCTP is complex and requires high computational effort. The computation time of the proposed approach can be further greatly reduced through parallel computation. The proposed approach could be also tested with other existing alternative OLCTP formulations. PE revealed that the instability risk may not be fully eliminated under wide-ranging operating conditions by considering a unique solution of OLCTP. Hence, an adaptive controller coordination scheme has been suggested to solve the task of real-time adaptation of system uncertainties in order to achieve robust damping control objectives.

V. REFERENCES

[1] Z. Huang, N. Zhou, F. Tuffner, Y. Chen, D. Trudnowski, W. Mittelstadt, J. Hauer, and J. Dagle, "Improving small signal stability through operating point adjustment," in *Proc. 2010 IEEE Power and Energy Society General Meeting*, pp. 1 – 8.

[2] M. R. Aghamohammadi, and A. Beik-Khormizi, "Small signal stability constrained rescheduling using sensitivities analysis by Neural Network as a preventive tool," in *Proc. 2010 IEEE PES Transmission and Distribution Conference and Exposition*, pp. 1-5.

[3] Y. Li, and V. Venkatasubramanian, " Coordination of transmission path transfers," *IEEE Transactions on Power Systems*, vol. 19, no. 3, pp. 1607-1615, Aug. 2004.
[4] J. Condren, and T. W. Gedra, "Expected-security-cost optimal power flow with small-signal stability constraints," *IEEE Transactions on Power Systems*, vol. 21, no. 4, pp. 1736-1743, Nov. 2006.
[5] S.P. Teeuwsen, I. Erlich, and M.A. El-Sharkawi, "Methods for estimation of counter measures to improve oscillatory stability in power systems", in *Proc. 15th Power Systems Computation Conference*, Liege, Belgium, Aug. 2005.
[6] P. Zhang, and A.H. Coonick, "Coordinated synthesis of PSS parameters in multi-machine power systems using the method of inequalities applied to genetic algorithms," *IEEE Trans. on Power Systems*, vol. 15, no. 2, pp. 811-816, May 2000.
[7] L. Qisheng, Y. Zhijuan, H. Xiaobo, L. Hong, "Study on the Selection of PSS Installing Locations in Power Systems," in *Proc. 2005 IEEE/PES Transmission and Distribution Conference and Exhibition: Asia and Pacific*, pp. 1-4.
[8] A. Karimpour, R. Asgharian, and O. P. Malik, "Determination of PSS location based on singular value decomposition," *International Journal of Electrical Power & Energy Systems*, vol. 27, no 8, pp. 535-541, May. 2005.
[9] F.L. Pagola, I.J. Perez-Arriaga, and G.C. Verghese, "On sensitivities, residues and participations: applications to oscillatory stability analysis and control," *IEEE Transactions on Power Systems*, vol. 4, no. 1, pp. 278 - 285, Feb. 1989.
[10] H.F. Wang, F.J. Swift, and M. Li, "Indices for selecting the best location of PSSs or FACTS-based stabilisers in multimachine power systems: a comparative study," *IEE Proceedings Generation, Transmission and Distribution*, vol. 4, no. 2, pp. 155 - 159, March 1997,
[11] C.Y. Chung, K.W. Wang, C.T. Tse, X.Y. Bian, and A.K. David, "Probabilistic eigenvalue sensitivity analysis and PSS design in multimachine systems," *IEEE Transactions on Power Systems*, vol. 18, no. 4, pp. 1439 - 1445, Nov. 2003.
[12] J.L. Rueda, and D.G. Colomé, "Comparative study of probabilistic methodologies for small signal stability assessmen," in *Proc. 8th CLAGTEE - Latin-American Congress on Electricity Generation and Transmission,* Oct. 2009.
[13] J.C.R. Ferraz, N. Martins, and G.N. Taranto, "A synthetic system for the robustness assessment of power system stabilizers," in *Proc. 2004 IEEE PES Power Systems Conference and Exposition*, vol. 2, pp. 1164 - 1170.
[14] N. Nallathambi, and P.N. Neelakantan, "Fuzzy logic based power system stabilizer," in *Proc. 2004 E-Tech*, vol. 2, pp. 68 - 73.
[15] P. Tulpule, and A. Feliachi, "Online learning neural network based PSS with adaptive training parameters," in *Proc. 2007 IEEE PES General Meeting*, vol. 2, pp. 1 - 7.
[16] A. Hashmani, and I. Erlich, "Power system stabilizer by using supplementary remote signals," in *Proc. 16th Power Systems Computation Conference*, Glasgow, Scotland, July 2008.
[17] B. Selvabala, and D. Devaraj, "Coordinated tuning of AVR-PSS using differential evolution algorithm," in *Proc. 2010 IPEC*, pp. 439 - 444, 2010.
[18] D. Canever, M.V. Cazzol, and E. Gaglioti, "A comprehensive tool for evaluation of critical electromechanical oscillation modes in very large power systems with optimal location and tuning of PSS," in *Proc. 2005 IEEE Russia Power Tech*, pp. 1-7.
[19] K. Sebaa, and M. Boudour, "Optimal locations and tuning of robust power system stabilizer using genetic algorithms," *Electric Power Systems Research*, vol. 79, no. 2, pp. 406 - 416, Feb. 2009.
[20] K. Sebaa, H. Guéguen, M. Boudour, "Mixed integer non-linear programming via the cross-entropy approach for power system stabilisers location and tuning," *IET Generation, Transmission & Distribution*, vol. 4, no. 8, pp. 928 - 939, 2010.
[21] J.L. Rueda, D.G. Colomé, and I. Erlich, "Assessment and enhancement of small signal stability considering uncertainties," *IEEE Transactions on Power Systems*, vol. 24, no. 1, pp. 198 – 207, Feb. 2009.
[22] J. Machowski, J. Bialek, and J. Bumby, *Power system dynamics: Stability and control*. New York: John Wiley & Sons, 2008.
[23] I. Jollife, Principal Component Analysis, 2nd. Edition, Springer, 2002.
[24] C.L.T. Borges, E.R.C. Viveros, and G.N. Taranto, " Parallel Genetic Algorithms Applied to Damping Controllers Tuning on a Linux Clusters of PCs," *WSEAS Transactions on Systems*, vol. 3, no. 3, pp. 1280 – 1285, 2001.
[25] A. Mendonca, and J.A.P. Lopes, "Robust tuning of PSS in power systems with different operating conditions," in *Proc. 2003 IEEE Bologna Power Tech Conference*.
[26] I. Erlich, G. K. Venayagamoorthy, and W. Nakawiro, " A mean-variance optimization algorithm," in *Proc. 2010 IEEE World Congress on Computational Intelligence, Barcelona, Spain*.
[27] I. Erlich, W. Nakawiro, and M. Martinez, "Optimal Dispatch of Reactive Sources in Wind Farms," in *Proc. 2011 IEEE PES General Meeting, Detroit, USA*.
[28] W. Nakawiro, I. Erlich, and J.L. Rueda, "A novel optimization algorithm for optimal reactive power dispatch: A comparative study," in *Proc. 4th International Conference on Electric Utility Deregulation and Restructuring and Power Technologies, Weihai, Shandong, China, July 2011*.
[29] D. Zimmerman, "MATPOWER", PSERC. [Online]. Software Available at: http://www.pserc.cornell.edu/matpower.
[30] M. A. Pai, *Energy Function Analysis for Power System Stability*, Kluwer Academic Publishers, 1989.
[31] "Standard PSO 2007 (SPSO-2007) on the Particle Swarm Central", [Online]. http://www.particleswarm.info, 2007.

VI. BIOGRAPHIES

José L. Rueda (M'07) was born in 1980. He received the Electrical Engineer diploma from the Escuela Politécnica Nacional, Quito, Ecuador, in 2004, and the Ph.D. degree in electrical engineering from the Universidad Nacional de San Juan, San Juan, Argentina, in 2009. From September 2003 till February 2005, he worked in Ecuador, in the fields of industrial control systems and electrical distribution networks operation and planning. Currently, he is a research associate at the Institute of Electrical Power Systems, University Duisburg-Essen. His current research interests include power system stability and control, system identification, power system planning, probabilistic and artificial intelligent methods, and wind power.

Jaime C. Cepeda (GSM'10) was born in 1981. He got his Electrical Engineer degree in 2005 from Escuela Politécnica Nacional, Quito, Ecuador. He is currently a Ph.D. candidate at Instituto de Energía Eléctrica, Universidad Nacional de San Juan, San Juan, Argentina, favored with a scholarship from the German Academic Exchange Service (DAAD). His research experience includes an internship at Institute of Electrical Power Systems, University Duisburg-Essen, Duisburg, Germany, as part of the DAAD scholarship. His special fields of interest comprise power system stability analysis, security assessment, and vulnerability assessment.

István Erlich (SM'08) was born in 1953. He received the Dipl.-Ing. degree in electrical engineering and the Ph.D. degree from the University of Dresden, Dresden, Germany, in 1976 and 1983, respectively. From 1979 to 1991, he was with the Department of Electrical Power Systems of the University of Dresden. In the period of 1991 to 1998, he worked with the consulting company EAB, Berlin, Germany, and the Fraunhofer Institute IITB Dresden. During this time, he also had a teaching assignment at the University of Dresden. Since 1998, he has been a Professor and head of the Institute of Electrical Power Systems at the University of Duisburg-Essen, Duisburg. Germany. His major scientific interest comprises power system stability and control, modeling, and simulation of power system dynamics, including intelligent system applications. Dr. Erlich is a member of VDE and the chairman of the IFAC (International Federation of Automatic Control) Technical Committee on Power Plants and Power Systems.